Chemical Engineering Journal 147 (2009) 336–341

Contents lists available at ScienceDirect

Chemical Engineering Journal

journal homepage: www.elsevier.com/locate/cej

Simulation of solid oxide fuel cell systems integrated with sequential CaO–CO_2 capture unit

S. Vivanpatarakij[a], N. Laosiripojana[b], W. Kiatkittipong[c], A. Arpornwichanop[a], A. Soottitantawat[a], S. Assabumrungrat[a,*]

[a] Department of Chemical Engineering, Faculty of Engineering, Chulalongkorn University, Bangkok 10330, Thailand
[b] The Joint Graduate School of Energy and Environment, King Mongkut's University of Technology Thonburi, Bangkok 10140, Thailand
[c] Department of Chemical Engineering, Faculty of Engineering and Industrial Technology, Silpakorn University, Nakhon Pathom 73000, Thailand

ARTICLE INFO

Article history:
Received 17 July 2008
Received in revised form
14 November 2008
Accepted 25 November 2008

Keywords:
Adsorption
CO_2 capture
Fuel cell system
SOFC

ABSTRACT

This paper presents preliminary simulation results from the performance analysis of the integrated systems of calcium oxide (CaO)–carbon dioxide (CO_2) capture unit and solid oxide fuel cell (SOFC). The CO_2 was extracted for further sequestration in the CaO–CO_2 capture unit. Three configurations of the integrated systems (CaO-Before-SOFC: CBS, CaO-After-SOFC: CAS and CaO-After-Burner: CAB) were considered. It was found that the CO_2 capture efficiency (E_c) is dependent on CaO fresh feed rate (F_0) and CaO recycle rate (F_R). The improvement of SOFC performance was only realized for the CBS system. The SOFC performance increases with increasing CO_2 E_c. The preliminary economic analysis was carried out considering total additional cost per mole of CO_2 captured. At a low percentage of CO_2 capture (<42.5%), the CBS system is the most suitable configuration while the CAS system becomes an attractive choice at higher values. However, only the CAB system could be possible at a very high range of CO_2 capture (>94%).

1. Introduction

Nowadays, global warming is considered to be an important problem of the world. A major cause is arisen from a large emission of carbon dioxide to the environment which has been particularly driven by the growth of economics. Therefore, low-CO_2-emission processes are desired. Fuel cell is one of the novel processes for electrical power generation via an electrochemical reaction of hydrogen. Small amount of CO_2 is emitted from the fuel cell. Among a various type of fuel cell, solid oxide fuel cell (SOFC) is the most promising process. Due to high electrical efficiency of SOFC, lower amount of fuel is consumed, resulting in a lower amount of generated CO_2. At present, a number of efforts have been carried out to improve its efficiency. An integration of an SOFC with a CaO–CO_2 capture unit is one of an attractive choice for electrical power generation. The use of the CaO–CO_2 capture unit for CO_2 sequestration could further reduce the amount of CO_2 emitted to the environment.

The in situ CaO–CO_2 capture for shifting equilibrium of reaction was studied [1–6]. A coal/H_2O/CaO gasification system offers a higher yield of hydrogen production compared to a conventional coal/H_2O gasification system [1]. Methane steam reforming reaction (MSR) combined with CaO-carbonation showed a potential benefit on CO_2 acceptor and hydrogen production at 1023 K [2]. The simulation of in situ carbonation of CaO in MSR was studied [3,4] and the kinetics of the carbonation of CaO were proposed. The addition of CaO in a methane steam reforming system can increase the purity of hydrogen to be higher than 95% in a laboratory-scale operation [5]. The similar result was also reported in an ethanol steam reforming with addition of CaO [6].

Although CaO is a good candidate for CO_2 capture, the main problem of CaO–CO_2 capture is the generation of $CaCO_3$. Therefore, a carbonation–calcination cycle of CaO was considered as reported in many researches [7–10]. Gupta and Fan [7] used the reaction based on the cycle of separated CO_2 with CaO from flue gas. Sintering of CaO sorbent was not observed within 2–3 cycles of carbonation–calcination at 973 K. However, carbonation conversion decreased with increasing the number of cycles [8,9]. Abanades [10] proposed an expression for calculating the maximum CO_2 capture efficiency of CaO.

Some researchers have investigated the combined system of fuel cell and CO_2 capture unit to improve the system efficiency and reduce the global warming gas. Amorelli et al. [11] reported that a 1.6 MW MCFC-gas turbine (MCFC/GT) incorporated with a CO_2 capture unit could reduce the CO_2 emission by 50% from the conventional MCFC/GT system. Moreover, Fredriksson Möller et al. [12] showed that an SOFC/GT system can be operated at an electrical efficiency close to 65% when incorporating with a CO_2 capture unit.

* Corresponding author. Tel.: +66 2 218 6868; fax: +66 2 218 6877.
E-mail address: Suttichai.A@chula.ac.th (S. Assabumrungrat).

1385-8947/$ – see front matter © 2008 Elsevier B.V. All rights reserved.
doi:10.1016/j.cej.2008.11.040

Nomenclature

a_j	constant in Eq. (11) (Ω m)
b	constant in Eq. (4) (0.174)
b_j	constant in Eq. (11) (K)
d_p	particle diameter (m)
D	diameter of reactor (m)
E	open circuit voltage (OCV) (V)
E_c	CO_2 capture efficiency (%)
E_0	reversible potential (V)
f	constant in Eq. (4) (0.782)
f_g	gas friction factor [14]
f_s	solid friction factor [14]
F	Faraday constant (96,485.34) (C mol^{-1})
F_0	fresh feed rate of CaO (mol s^{-1})
F_{CO_2}	molar flow rate of CO_2 (mol s^{-1})
F_R	recycle rate of CaO (mol s^{-1})
g	gravity acceleration (m s^{-2})
i	current density (A m^{-2})
i_0	exchange current density (A m^{-2})
L	length of reactor (m)
m	exponent parameter in Eq. (15)
n_e	number of electron transfer
P	total pressure (atm)
P_i	partial pressure (atm)
R	universal gas constant (8.31447×10^{-3}) (kJ mol^{-1} K^{-1})
T	absolute temperature (K)
u	velocity (m s^{-1})
U_f	fuel utilization (%)
v_t	gas terminal velocity (m s^{-1})
V	operating voltage (V)

Greeks letters

α	electron transfer coefficient
δ	thickness (m)
ε	bed void fraction
η_i	overpotential (Ω m^2)
μ	viscosity of fluid (Pa s)
ρ	density (kg m^{-3})
ρ_ι	specific ohmic resistance (Ω m)

Subscript

A	anode
C	cathode
f	fluid
p	particle

In this study, performances of various systems of SOFC integrated with carbonation–calcination systems (SOFC–CaO system) were simulated. The effects of location of CaO–CO_2 acceptor in the SOFC system, the CaO fresh feed rate, the CaO recycle rate and the fuel utilization were studied in terms of amount of CO_2 captured and SOFC performance. Finally, preliminary economic analysis was also considered.

2. Theory

2.1. Methane steam reforming

Methane steam reforming is the conventional route for hydrogen production. The major reactions taking place in the reactor are methane steam reforming (MSR, Eq. (1)) and water gas shift reaction (WGSR, Eq. (2)).

$$CH_4 + H_2O \leftrightarrows CO + 3H_2 \quad (1)$$

$$CO + H_2O \leftrightarrows CO_2 + H_2 \quad (2)$$

$$CH_4 + 2H_2O \leftrightarrows CO_2 + 4H_2 \quad (3)$$

In order to avoid a carbon formation problem, the molar ratio of H_2O:CH_4 in the feed stream should be higher than 2.5 [13]. In this work, it was assumed that the gas exiting the reformer is at its equilibrium composition.

2.2. CaO–CO_2 acceptor systems

Carbonation reaction of calcium oxide (CaO) can convert carbon dioxide (CO_2) to calcium carbonate ($CaCO_3$) whereas $CaCO_3$ can reverse to CaO at high temperature calcinations. The carbonation–calcination cycle for CO_2 separation is illustrated in Fig. 1. The maximum efficiency of CO_2 capture can be expressed as follows [10]:

$$E_c = \frac{F_R + F_0}{F_0 + F_{CO_2}} \cdot \left(\frac{f \cdot F_0}{F_0 + F_R(1-f)} + b \right) \quad (4)$$

where $b = 0.174$, $f = 0.782$, F_0 is fresh feed rate of CaO, F_R is feed recycle rate of CaO and F_{CO_2} is feed rate of CO_2.

The circulating fluidized bed was chosen for the CaO carbonation–calcination operation. The constraint of circulating fluidized bed is that gas velocity (v) must be higher than gas terminal velocity (v_t), ($v > v_t$) (Eq. (5)). Pressure drop along the reactor can be calculated by Eq. (6) [14].

$$v_t = \frac{g(\rho_p - \rho_f)d_p^2}{18\mu} \quad (5)$$

$$\frac{\Delta P}{L} = \rho_p(1-\varepsilon)g + \rho_f \varepsilon g + \frac{2f_g \rho_f u_f^2}{D} + \frac{2f_s \rho_p (1-\varepsilon) u_p^2}{D} \quad (6)$$

2.3. SOFC

An SOFC unit consists of two porous ceramic electrodes (i.e., an anode and a cathode) and a solid ceramic electrolyte. In theory, both hydrogen and CO can react electrochemically with oxygen ions at the anode of the SOFC cells. However, it was reported that about 98% of current is produced via H_2 oxidation in common situations [15]. Therefore it was assumed in this study that the CO electro-oxidation is neglected. The theoretical open-circuit voltage of the cell (E), which is the maximum voltage under specific operating conditions, can be calculated from the following equations [16]:

$$E = E_0 + \frac{RT}{2F} \ln \left(\frac{P_{H_2} P_{O_2}^{0.5}}{P_{H_2O}} \right) \quad (7)$$

$$E_0 = 1.253 - 2.4516 \times 10^{-4} T \quad (8)$$

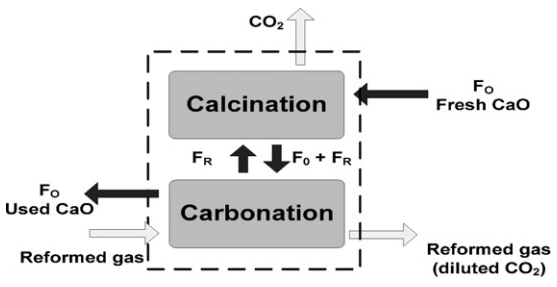

Fig. 1. Schematic diagram of a CaO–CO_2 acceptor system.

The actual voltage (Eq. (9)) is usually lower than the theoretical open-circuit voltage due to the presence of polarization losses: ohmic polarization, activation polarization and concentration polarization [17].

$$V = E - (\eta_{Ohm} + \eta_{Act} + \eta_{Conc}) \quad (9)$$

The ohmic polarization (Eqs. (10) and (11)) is the resistance of electrons through electrolyte and that of ions through electrodes. The activation polarization (Eqs. (12)–(15)) is mostly illustration of a loss for driving the electrochemical reaction to completion. The concentration polarization occurs due to the mass transfer limitation through the porous electrodes.

Ohmic polarization:

$$\eta_{Ohm} = \sum \rho_j \delta_j \quad (10)$$

$$\rho_j = a_j \exp(b_j T) \quad (11)$$

Activation polarization:

$$i = i_0 \left[\exp\left(\frac{\alpha n_e F \eta_{Act}}{RT}\right) - \exp\left(-\frac{(1-\alpha) n_e F \eta_{Act}}{RT}\right)\right] \quad (12)$$

$$\eta_{Act} = \frac{2RT}{n_e F} sinh^{-1}\left(\frac{i}{i_0}\right); \quad \text{where } \alpha = 0.5 \quad (13)$$

$$i_{0,A} = 5.5 \times 10^8 \left(\frac{p_{H_2}}{p}\right)\left(\frac{p_{H_2O}}{p}\right) \exp\left(\frac{-100 \times 10^3}{RT}\right) \quad (14)$$

$$i_{0,C} = 7.0 \times 10^8 \left(\frac{p_{O_2}}{p}\right)^m \exp\left(\frac{-120 \times 10^3}{RT}\right) \quad (15)$$

To simplify the calculation of the SOFC performance, it was assumed that both fuel and oxidant are well-diffused through the electrodes. Therefore, the concentration polarization losses ($\eta_{Conc,A}$ and $\eta_{Conc,C}$) are neglected. This assumption is valid when the current density is not very high [18]. Table 1 summarizes the ohmic polarization parameters of the cell components employed in this work. It was also assumed that the gas composition in the anode is always at its equilibrium as the rate of WGSR is fast particularly at high operating temperatures of SOFC [15]. The model validations of methane steam reformer and fuel cell performance were performed and good agreements with previous literatures [16,19] were observed.

Table 1
Ohmic polarization constants of Eqs. (10) and (11).

	a	b	δ (μm)
Anode (Ni–YSZ)	2.98×10^{-5}	−1,392	50
Cathode (LSM–YSZ)	8.11×10^{-5}	600	50
Electrolyte (YSZ)	2.94×10^{-5}	10,350	140

2.4. CaO–SOFC configurations

The conventional SOFC system is composed of a reformer, an SOFC and an afterburner. First, methane and water are fed to the reformer where methane steam reforming reaction and water gas shift reaction take place. Then, the reformed gas, a mixture of hydrogen, carbon monoxide, carbon dioxide and unreacted reagents, are fed to the SOFC unit. Oxygen is reduced, permeated through an electrolyte and then reacted with hydrogen at the anode. After that, the exhaust gas is fed to the afterburner where residual fuels are combusted, providing heat to other parts of the system. Fig. 2(a–c) shows the SOFC systems with different configurations: (a) the SOFC system incorporated with a CaO–CO_2 acceptor before the SOFC unit (CaO-Before-SOFC: CBS), (b) the SOFC system incorporated with a CaO–CO_2 acceptor after the SOFC unit (CaO-After-SOFC: CAS) and (c) the SOFC system incorporated with a CaO–CO_2 acceptor after the afterburner unit (CaO-After-Burner: CAB). Because the amount of CO_2 produced varies among the different streams in the system, the location of the CaO–CO_2 capture unit could affect the performance of the SOFC system. Table 2 summarizes the standard operating condition of the SOFC with the CaO–CO_2 acceptor.

2.5. Economic analysis

Economic analysis was carried out to compare the costs of different SOFC systems incorporated with a sequential CaO–CO_2 capture unit. The total capital cost includes the costs of compressor, SOFC stack (1500 \$/m^2) [18] and CaO (60 \$/ton). The compressor cost was

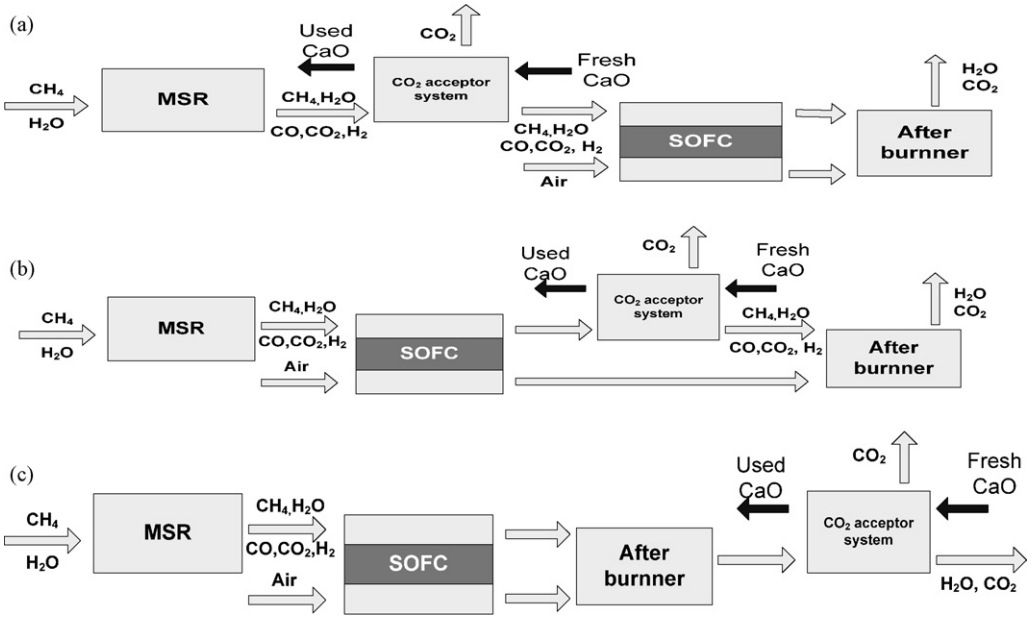

Fig. 2. Schematic diagrams of (a) CBS system, (b) CAS system and (c) CAB system.

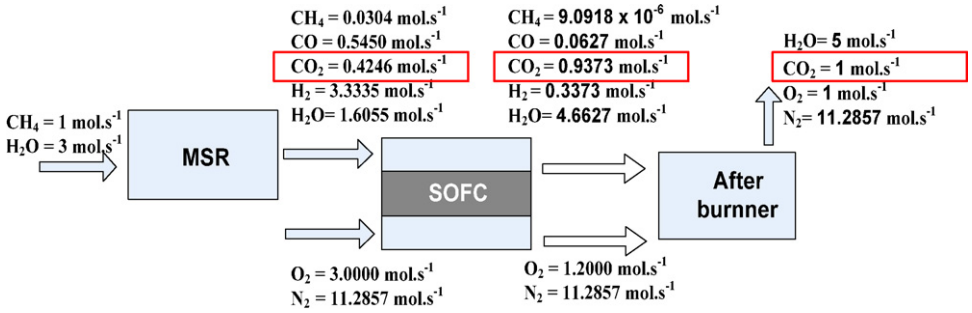

Fig. 3. Molar flow rates of different gases in the conventional SOFC system (U_f = 90%, T_R = 973 K and T_{SOFC} = 1073 K).

estimated from the following expression [20]:

$$\text{Cost of compressor (\$)} = 1.49 \cdot \text{HP}^{0.71} \times 10^3 \quad (16)$$

where 10 < HP < 800.

3. Results and discussion

Fig. 3 shows molar flow rates of different gases in the conventional SOFC system operated at U_f = 90%, T_R = 973 K and T_{SOFC} = 1073 K. Methane of 1 mol s^{-1} and water of 3 mol s^{-1} were fed to the system. The CO_2 flow rates of the streams before SOFC, after SOFC and after the burner are 0.4246, 0.9373 and 1.0 mol s^{-1}, respectively. Therefore, different amount of CO_2 can be captured when the CaO–CO_2 acceptor is installed at different places in the system. The flow rate of CO_2 after the reformer (before the SOFC) is still low as the WGSR is a mildly exothermic and therefore CO is not favorably converted to CO_2 at this high reforming temperature (973 K). The flow rate of CO_2 increases in the SOFC as hydrogen is consumed, generating H_2O which can further convert CO to CO_2 by WGSR in the anode channel. Finally, the flow rate of CO_2 becomes the highest after all spent fuels are completely combusted in the afterburner.

The effects of fresh CaO feed (F_0) and recycle rate of CaO (F_R) on maximum CO_2 capture efficiency (E_c) for the CBS, CAS and CAB systems are shown in Fig. 4(a–c). As indicated in Eq. (4), the maximum CO_2 capture efficiency (E_c) depends on the flow rate of fresh CaO feed (F_0), the recycle rate of CaO (F_R) and the concentration of CO_2 in the stream inlet. All figures show that the CO_2 capture efficiency increases with increasing fresh CaO feed (F_0) and recycle rate of used CaO (F_R). Therefore, a higher E_c can be achieved by increasing F_0 and/or F_R.

The SOFC performance in the case of CBS at various values of fuel utilization (U_f) and CO_2 capture efficiency (E_c) is illustrated in Fig. 5. Solid lines represent the obtained power density of the conventional SOFC system while dashed lines represent the power density at different values of E_c ranging from 50 to 90%. It is obvious that the CBS can improve the SOFC performance. This is particularly pronounced at a higher efficiency of CO_2 capture. It should be noted that the SOFC performance improvement is not realized in the CAS and CAB systems as the feed composition of the SOFC is not

Table 2
Standard condition.

Parameter	Value
CH_4 feed rate	1 (mol s^{-1})
H_2O:CH_4 feed ratio	3 (–)
Temperature of SOFC (T_{SOFC})	1073 (K)
Temperature of reformer (T_R)	973 (K)
Temperature of carbonation of CaO	873 (K)
Temperature of calcination of $CaCO_3$	1173 (K)
Air:CH_4 feed ratio	15 (–)
Temperature of reformer (T_R)	973 (K)
Density of CaO (ρ_{CaO})	1503 (kg m^{-3})
Bed void fraction (ε)	0.45 (–)
Particle size of CaO	0.5 (mm)
Length:diameter ratio of CaO acceptor (L/D)	10 (–)

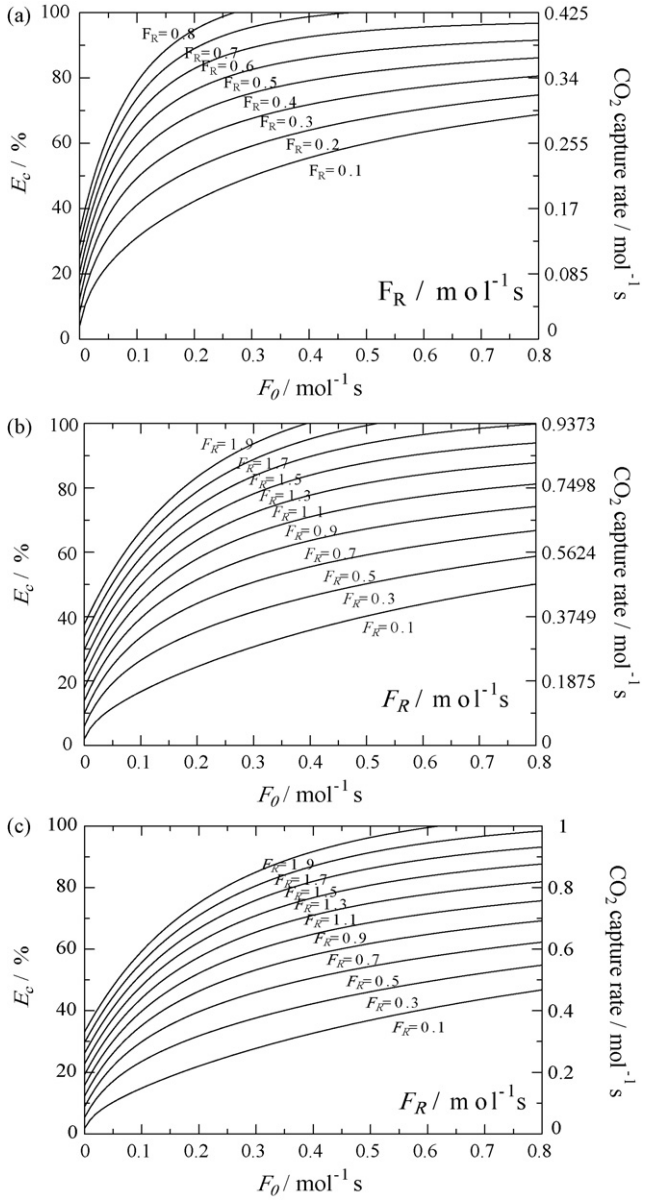

Fig. 4. Effects of CaO fresh feed rate (F_0) and CaO recycle rate (F_R) on CO_2 capture efficiency (E_c): (a) CBS, (b) CAS and (c) CAB (T_R = 973 K).

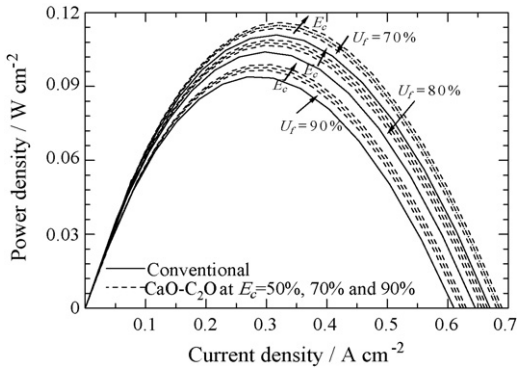

Fig. 5. Comparison of SOFC performance between CBS and conventional SOFC systems at various values of CO_2 capture efficiency (E_c) and fuel utilization (U_f) (T_R = 973 K, T_{SOFC} = 1073 K).

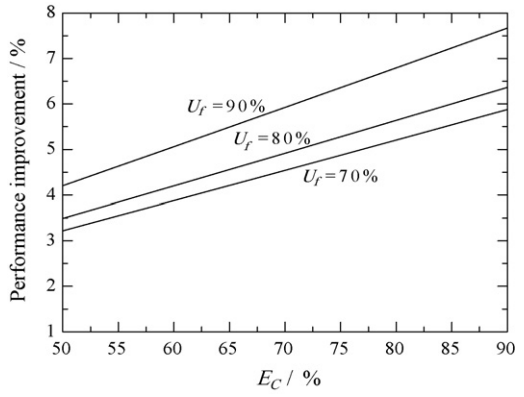

Fig. 6. Performance improvement of CBS system (V = 0.56 V, T_R = 973 K, T_{SOFC} = 1073 K).

influenced by the presence of the CaO–CO_2 acceptor. Therefore, the SOFC performance of CAS and CAB system is not different from the conventional system without the CaO–CO_2 acceptor. Fig. 6 shows the SOFC performance improvement for the CBS system in term of power density compared to that of the conventional system. The SOFC performance increases with increasing the fuel utilization and efficiency of CO_2 capture. With E_c = 90% and U_f = 90%, the CBS can increase the performance of SOFC by 8%.

A preliminary economic analysis of different SOFC–CaO systems was carried out to determine a suitable place of the CaO–CO_2 capture unit to be integrated in the SOFC system. With the presence of the capture unit, some electrical power is required to operate the compressor for fluidizing the CaO adsorbent. Furthermore, there is the additional operating cost on the use of fresh CaO. In order to achieve a minimum cost on compressor and compressor power, it is desired to operate the CaO–CO_2 capture unit at the condition in which the total flow rate of CaO in the capture unit ($F_0 + F_R$) is at minimum. Fig. 7 shows an example for determining a suitable F_0 for the case of CBS. It is observed that the optimum F_0 increases with the increasing CO_2 capture efficiency (E_c). The other systems were also calculated on the same procedure. For comparison among the different systems, total additional cost from the use of CaO–CO_2 capture unit, which was assumed to be operated for 5 years, was calculated taking into account the capital cost (extra SOFC area and compressor) and the operating cost (cost of CaO). Table 3 shows an example of the economic analysis for the systems with net electrical power of about 400 kW (electrical efficiency = 45.9%) and %CO_2 capture of 38.2%. It is observed that additional electrical power required for operating the compressor in CAB systems is higher than the CBS and CAS systems about 5 times. As the CO_2 composition in the exhaust gas from the afterburner is much lower than that of the reformed gas and the anode gas from the SOFC, much higher electrical power is required. Furthermore, the CAB system also showed the highest requirement of SOFC area which is about twice of the other systems. This is corresponding well with the required electrical power. It should be noted that for the CBS system, a lower SOFC area compared to that of the conventional SOFC system is observed due to the improved SOFC performance as discussed earlier. From

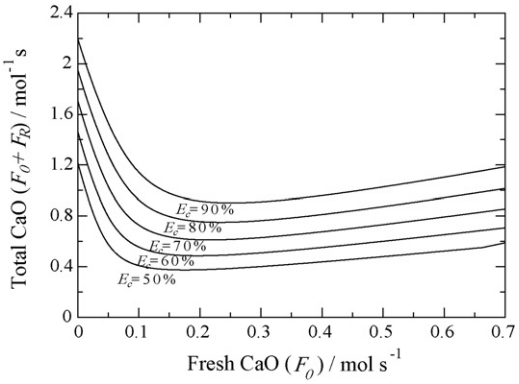

Fig. 7. Effect of CaO fresh feed rate on total in-process CaO flow rate ($F_0 + F_R$) for the CAS system (T_R = 973 K).

Table 3
Economic analysis of CaO–SOFC system and conventional SOFC system.

	Conventional	CBS	CAS	CAB
CO_2 reduction (%)	–	38.2	38.2	38.2
Fuel utilization (U_f) (%)	90	90	90	90
Total electrical power production (kW)	401.39	401.39	401.39	401.39
Total electrical efficiency (%)	45.9	45.9	45.9	45.9
Electrical power (kW)	401.39	408.53	409.5	440.07
SOFC area (m^2)	723.86	719.24	794.59	1,406.06
Compressor power (kW)	–	7.14	8.11	38.69
Operating voltage (V)	0.58	0.59	0.59	0.63
Cost of SOFC area/\$ (1500 \$ m^{-2})	1,085,784	1,078,860	1,191,882	2,109,086
Compressor cost (\$)	–	6,018.95	6,585.89	19,969.23
Additional SOFC cost (\$)	–	−6,924	106,097	1,023,301
F_R of CaO (mol s^{-1})	–	0.65269	0.29982	0.28209
F_0 of CaO (mol s^{-1})	–	0.25	0.335	0.34
Total CaO at start up (mol)	–	0.90269	0.63482	0.62209
Operating cost of capture unit: 5 years/\$	–	132,639	177,736	180,389
Total additional cost (\$)	–	125,715	283,833	1,203,690
CO_2 reduction: 5 years/mol	–	66.9×10^6	66.9×10^6	66.9×10^6
Total additional cost:mol of CO_2 captured (\$ mol^{-1})	NA	0.0019	0.0042	0.0180

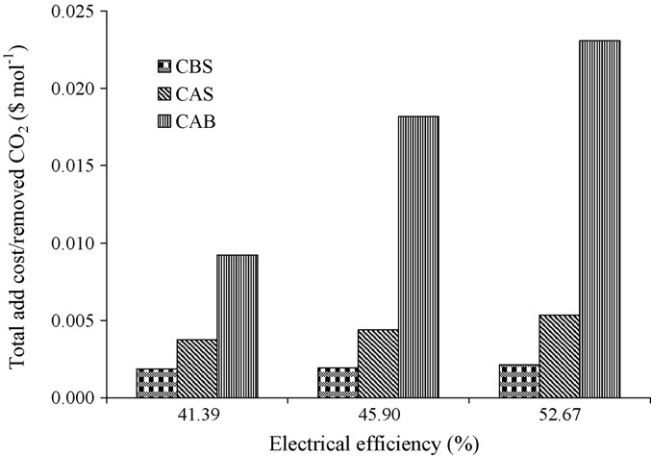

Fig. 8. Effect of electrical efficiency on total additional cost per mole of CO_2 captured (U_f = 90%, T_{SOFC} = 1073 K, CO_2 capture rate = 0.382 mol s^{-1}).

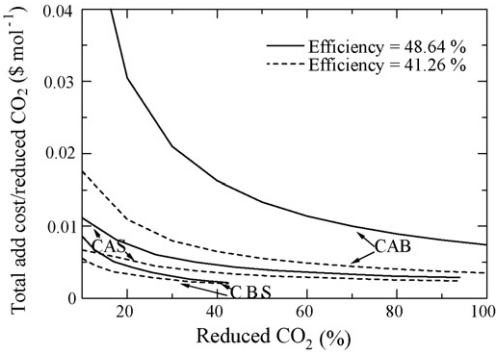

Fig. 9. Economic analysis of CBS, CAS and CAB system (T_R = 973 K, T_{SOFC} = 1073 K).

the comparison, it is observed that at 38.2% CO_2 capture the CBS system is the most attractive system due to the lowest total additional cost and total additional cost per mole of CO_2 captured.

Fig. 8 shows the total additional cost per mole of CO_2 captured at various values of electrical efficiency (41.4, 45.9 and 52.7%). It is obvious that the cost per mole of CO_2 captured increases when the overall system is operated at a higher electrical efficiency. However, the increase is much less pronounced for the CBS system having improved SOFC performance.

Fig. 9 shows the total additional cost per mole of CO_2 captured at various levels of CO_2 capture. The solid lines represent the case with an electrical efficiency of 48.6% while dash lines represent that with an electrical efficiency of 41.3%. It is obvious that for each level of %CO_2 capture, the additional cost per mole of CO_2 captured is in the order: CBS < CAS < CAB. However, the maximum %CO_2 capture varies among the systems. From the study it is suggested that at a low range of %CO_2 capture (<42.5%) the CBS system is the best configuration. At a higher range, the CAS system is recommended. However, at a very high value (>94%) the CAB system is the only possible configuration for operation. It should be noted that although the energy balance has not been considered in this study, our calculations indicate that the exothermic energy from the SOFC stack, the after-burner and the carbonation reaction is sufficient to provide the heat to the heat-consuming units in the integrated system such as the feed preheaters, the reformer and calcination reaction. In addition, for practical operation, design of a heat exchanger network for the integrated system of CaO–CO_2 capture unit and SOFC is required. The design needs to take into account the periodic operation nature of the CaO–CO_2 capture unit.

4. Conclusions

The SOFC system integrated with a CaO–CO_2 capture unit was investigated in this study. The effect of location of the CaO–CO_2 capture unit in the SOFC system (i.e., CaO-Before-SOFC; CBS, CaO-After-SOFC; CAS and CaO-After-Burner; CAB) and other operating parameters on the amount of CO_2 captured, SOFC performance and economic analysis was considered. It was found that all SOFC–CaO systems can reduce the CO_2 emission; however, only the CBS system can improve performance of SOFC. Economic analysis was carried out to compare the different systems. It was indicated that the additional cost per mole of CO_2 captured follows the order: CBS < CAS < CAB. However, the selection of a suitable system significantly depends on the level of CO_2 capture.

Acknowledgement

The support from The Thailand Research Fund and Commission on Higher Education is gratefully acknowledged.

References

[1] Z. Wang, J. Zhou, Q. Wang, J. Fan, K. Cen, Int. J. Hydrogen Energy 31 (2006) 945–952.
[2] D.K. Lee, I.H. Baek, W.L. Yoon, Chem. Eng. Sci. 59 (2004) 931–942.
[3] D.K. Lee, I.H. Baek, W.L. Yoon, Int. J. Hydrogen Energy 31 (2006) 649–657.
[4] D.K. Lee, Chem. Eng. J. 100 (2004) 71–77.
[5] B. Balasubramanian, A. Lopez Ortiz, S. Kaytakoglu, D.P. Harrison, Chem. Eng. Sci. 54 (1999) 3543–3552.
[6] J. Comas, M. Laborde, N. Amadeo, J. Power Sources 138 (2004) 61–67.
[7] H. Gupta, L.S. Fan, Ind. Eng. Chem. Res. 41 (2002) 4035–4042.
[8] M.V. Iyer, H. Gupta, B.B. Sakadjian, L.S. Fan, Ind. Eng. Chem. Res. 43 (2004) 3939–3947.
[9] G.S. Grasa, J.C. Abanades, M. Alonso, B. Gonzalez, Chem. Eng. J. 137 (2008) 561–567.
[10] J.C. Abanades, Chem. Eng. J. 90 (2002) 303–306.
[11] A. Amorelli, M.B. Wilkinson, P. Bedont, P. Capobianco, B. Marcenaro, F. Parodi, A. Torazza, Energy 29 (2004) 1279–1284.
[12] B. Fredriksson Möller, J. Arriagada, M. Assadi, I. Potts, J. Power Sources 131 (2004) 320–326.
[13] H.J. Renner, R. Marschner, Catalytic reforming of natural gas and other hydrocarbon Ullmann's Encyclopedia of Industrial Chemistry, vol. A2, fifth ed., VCH Verlagsgesellschaft, Weinheim, Germany, 1985, pp. 186–204.
[14] S.M. Walas, Chemical Process Equipment Selection and Design, Butterworth, Inc., 1988.
[15] M.A. Khaleel, Z. Lin, P. Singh, W. Surdoval, D. Collin, J. Power Sources 130 (2004) 136–148.
[16] E. Hernandez-Pacheco, M.D. Mann, P.N. Hutton, D. Singh, K.E. Martin, Int. J. Hydrogen Energy 30 (2005) 1221–1233.
[17] M. Pfafferodt, P. Heidebrecht, M. Stelter, K. Sundmacher, J. Power Sources 149 (2005) 53–62.
[18] E. Riensche, U. Stimming, G. Unverzagt, J. Power Sources 73 (1998) 251–256.
[19] J. Shu, B.P.A. Grandjean, S. Kaliaguine, Appl. Catal. A 119 (1994) 305–325.
[20] S.M. Walas, Chemical Process Equipment Selection and Design, Butterworth, Inc., 1988, pp. 665–668.